0026-895X/07/7202-463–476$20.00
MOLECULAR PHARMACOLOGY

Mol Pharmacol 72:463–476, 2007

Vol. 72, No. 2
37630/3238202
Printed in U.S.A.

Structure-Function Studies of Allosteric Agonism at M_2 Muscarinic Acetylcholine Receptors

Lauren T. May, Vimesh A. Avlani, Christopher J. Langmead, Hugh J. Herdon, Martyn D. Wood, Patrick M. Sexton, and Arthur Christopoulos

Drug Discovery Biology Laboratory, Department of Pharmacology, Monash University, Clayton, Victoria, Australia (L.T.M., V.A.A., P.M.S., A.C.) and Psychiatry Centre of Excellence for Drug Discovery, GlaxoSmithKline, Harlow, Essex, United Kingdom (C.J.L., H.J.H., M.D.W.)

Received April 30, 2007; accepted May 24, 2007

ABSTRACT

The M_2 muscarinic acetylcholine receptor (mAChR) possesses at least one binding site for allosteric modulators that is dependent on the residues ^{172}EDGE^{175}, Tyr^{177}, and Thr^{423}. However, the contribution of these residues to actions of allosteric agonists, as opposed to modulators, is unknown. We created mutant M_2 mAChRs in which the charge of the ^{172}EDGE^{175} sequence had been neutralized and each Tyr^{177} and Thr^{423} was substituted with alanine. Radioligand binding experiments revealed that these mutations had a profound inhibitory effect on the prototypical modulators gallamine, alcuronium, and heptane-1,7-bis-[dimethyl-3′-phthalimidopropyl]-ammonium bromide (C_7/3-phth) but minimal effects on the orthosteric antagonist [^{3}H]*N*-methyl scopolamine. In contrast, the allosteric agonists 4-*I*-[3-chlorophenyl]carbamoyloxy)-2-butynyltrimethylammnonium chloride (McN-A-343), 4-*n*-butyl-1-[4-(2-methylphenyl)-4-oxo-1-butyl] piperidine hydrogen chloride (AC-42), and the novel AC-42 derivative 1-[3-(4-butyl-1-piperidinyl)propyl]-3,4-dihydro-2(1*H*)-quinolinone (77-LH-28-1) demonstrated an increased affinity or proportion of high-affinity sites at the combined EDGE-YT mutation, indicating a different mode of binding to the prototypical modulators. Subsequent functional assays of extracellular signal-regulated kinase (ERK)1/2 phosphorylation and guanosine 5′-(γ-[^{35}S]thio)triphosphate ([^{35}S]GTPγS) binding revealed minimal effects of the mutations on the orthosteric agonists acetylcholine (ACh) and pilocarpine but a significant increase in the efficacy of McN-A-343 and potency of 77-LH-28-1. Additional mutagenesis experiments found that these effects were predominantly mediated by Tyr^{177} and Thr^{423}, rather than the ^{172}EDGE^{175} sequence. The functional interaction between each of the allosteric agonists and ACh was characterized by high negative cooperativity but was consistent with an increased allosteric agonist affinity at the combined EDGE-YT mutant M_2 mAChR. This study has thus revealed a differential role of critical allosteric site residues on the binding and function of allosteric agonists versus allosteric modulators of M_2 mAChRs.

Muscarinic acetylcholine receptors (mAChRs) are a group of five family A G protein-coupled receptors (GPCRs) distributed throughout the body (Hulme et al., 1990; Christopoulos, 2007). Drugs targeting mAChRs are currently used in the treatment of chronic obstructive pulmonary disease and urinary incontinence. These receptors also represent potential therapeutic targets for conditions such as Alzheimer's disease, schizophrenia, and irritable bowel syndrome (Felder et al., 2000; Eglen et al., 2001). To date, however, the widespread development of highly efficacious mAChR therapeutics with acceptable side effect profiles has been limited by a relative lack of ligands with sufficient subtype selectivity (Felder et al., 2000; Eglen et al., 2001).

Allosteric modulation of GPCRs represents a novel therapeutic avenue for overcoming difficulties associated with selective drug targeting (Christopoulos, 2002; May et al., 2007), and may be particularly amenable to mAChRs. Functional and radioligand binding studies have provided evidence for at least two allosteric binding sites on each mAChR subtype (Ellis et al., 1991; Christopoulos et al., 1998; Lazareno et al.,

This work was funded by project grant 400134 of the National Health and Medical Research Council (NHMRC) of Australia. A.C. is a Senior Research Fellow and P.M.S. is a Principal Research Fellow of the NHMRC.

Article, publication date, and citation information can be found at http://molpharm.aspetjournals.org.

doi:10.1124/mol.107.037630.

ABBREVIATIONS: mAChR, muscarinic acetylcholine receptor; GPCR, G protein-coupled receptor; ATCM, allosteric ternary complex model; McN-A-343, 4-(*N*-(3-chlorophenyl)carbamoyloxy)-2-butynyltrimethyl-ammonium chloride; AC-42, 4-*n*-butyl-1-[4-(2-methylphenyl)-4-oxo-1-butyl] piperidine hydrogen chloride; NMS, *N*-methylscopolamine; TM, transmembrane domain; 77-LH-28-1, 1-[3-(4-butyl-1-piperidinyl)propyl]-3,4-dihydro-2(1*H*)-quinolinone; DMEM, Dulbecco's modified Eagle's medium; FBS, fetal bovine serum; [^{35}S]GTPγS, guanosine 5′-(γ-[^{35}S]thio)triphosphate; C_7/3-phth, heptane-1,7-bis-[dimethyl-3′-phthalimidopropyl]-ammonium bromide; CHO, Chinese hamster ovary; Gpp(NH)p, guanosine 5′-(β,γ-imido)triphosphate; ERK1/2, extracellular signal regulated kinases 1 and 2.

2000), with one of the sites recognized by prototypical mAChR allosteric modulators, such as gallamine, alcuronium, and heptane-1,7-bis-[dimethyl-3′-phthalimidopropyl]-ammonium bromide (C_7/3-phth) (Lanzafame et al., 1997). The allosteric interactions mediated by these mAChR modulators are for the most part adequately described by a simple allosteric ternary complex model (ATCM) (Ehlert, 1988; Lazareno and Birdsall, 1995), with the effects of the modulators largely restricted to either enhancing or inhibiting orthosteric ligand binding affinity; minimal, if any, intrinsic efficacy has been detected for these compounds (but see Zahn et al., 2002).

It is now recognized, however, that some GPCR allosteric ligands have the capacity to affect receptor signaling in the absence of orthosteric agonist (Langmead and Christopoulos, 2006). Such "allosteric agonists" represent an important expansion in the chemical space surrounding allosteric modulators, because they have the potential to modulate orthosteric ligand pharmacology in addition to perturbing cellular signaling in their own right. Two mAChR ligands suggested to act this way are the functionally selective partial agonists McN-A-343 and AC-42 (Fig. 1A). Both compounds have been reported to cause incomplete inhibition of the binding of the orthosteric antagonist [^{3}H]*N*-methylscopolamine ([^{3}H]NMS) when present at saturating concentrations at rat M_2 (McN-A-343) and human M_1 (AC-42) mAChRs, as well as retarding [^{3}H]NMS dissociation (Birdsall et al., 1983; Waelbroeck, 1994; Langmead et al., 2006); these phenomena are characteristics of the formation of a ternary complex between the receptor and two concomitantly bound ligands. Despite these observations, it remains to be determined whether the allosteric effects of these agonists are receptor subtype- or species-dependent, what the relationship is between the common allosteric site recognized by prototypical modulators and that recognized by allosteric agonists, and whether both the agonistic and allosteric modulator properties of these latter

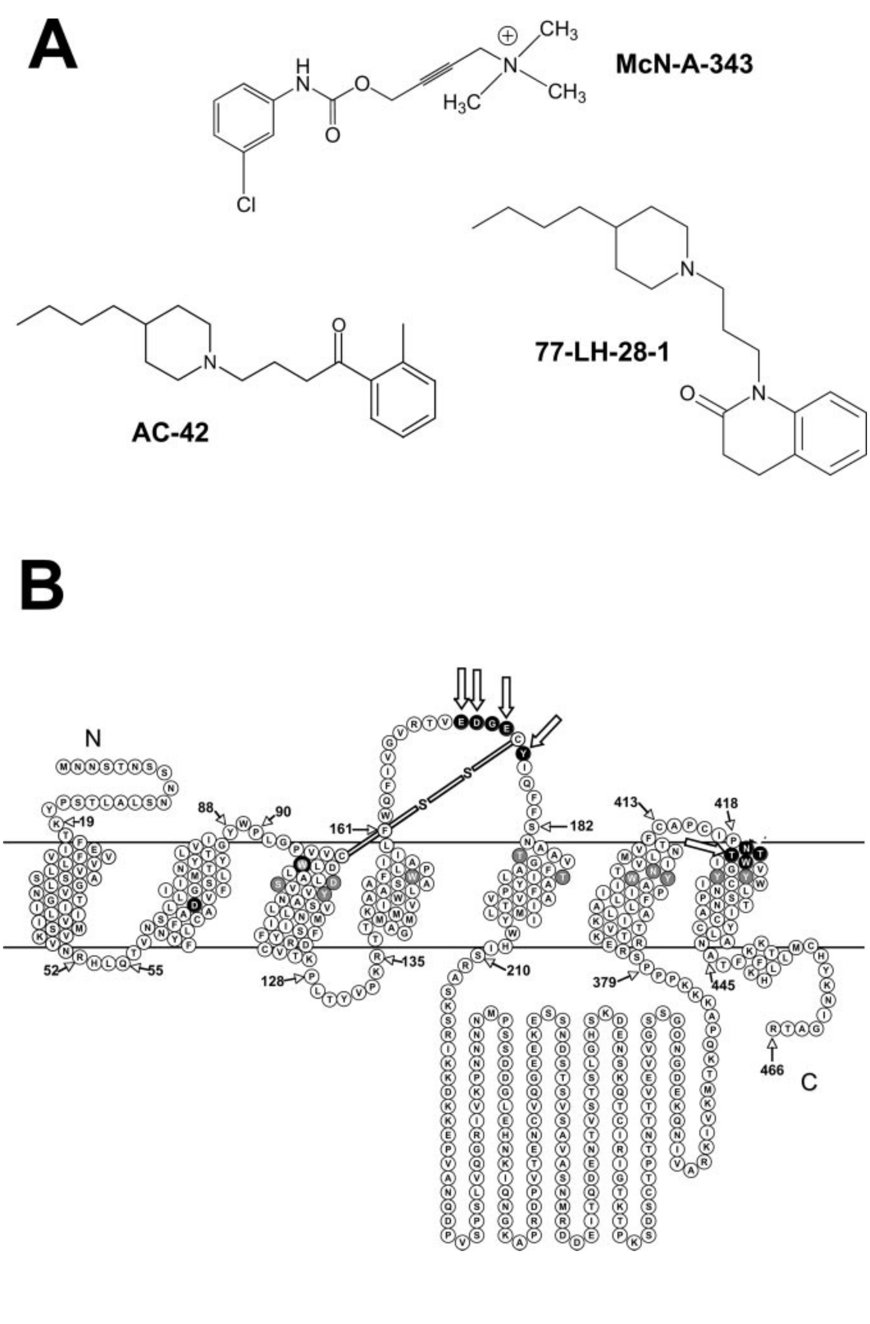

Fig. 1. A, structures of the allosteric mAChR agonists used in this study. B, snake diagram of the M_2 mAChR, indicating amino acids previously reported to contribute to orthosteric ligand binding (gray) and prototypical allosteric modulator binding (black). Amino acids highlighted by bold white arrows indicate those mutated in our current study.

compounds are mediated via the same (allosteric) domain on the receptor, or whether they reflect differential interactions with the orthosteric site (agonism) and an allosteric site (modulation).

Using the M_2 mAChR as a model, prior mutagenesis studies have found that the common allosteric site recognized by classic mAChR modulators comprises the second extracellular loop and the interface between the third extracellular loop and the top of transmembrane domain (TM) 7; specifically, the highly acidic ^{172}EDGE^{175} sequence (Leppik et al., 1994), as well as Tyr^{177} in the second extracellular loop, Asn^{419} at the junction of the third extracellular loop and TM7, and Thr^{423} near the top of TM7 (Fig. 1B) (Voigtländer et al., 2003; Huang et al., 2005). The conserved Trp^{422} in TM7 has also been implicated in the actions of allosteric modulators of mAChRs (Matsui et al., 1995; Prilla et al., 2006). It is noteworthy that most mutations in these regions that affect allosteric modulator binding have minimal effects on binding of orthosteric ligands.

In contrast to the studies on prototypical modulators, there have been no reports to date on the effect of allosteric site mutations on the actions of allosteric agonists. Thus, the aim of the current study was to investigate the mode of action of McN-A-343, AC-42, and a novel AC-42 derivative, 77-LH-28-1 (Fig. 1A), that we have recently found to be a more potent M_1-selective agonist than AC-42 (C. J. Langmead, C. Bock-Zeigler, C. L. Branch, J. T. Brown, K. A. Buchanan, C. H. Davies, I. T. Forbes, V. A. H. Fry, J. J. Hagan, H. J. Herdon, et al., manuscript in preparation) at the human M_2 mAChR, and to assess the contribution of the "common allosteric site" ^{172}EDGE^{175}, Tyr^{177}, and Thr^{423} epitopes of the M_2 mAChR on the pharmacology of these agents.

Materials and Methods

Materials. Dulbecco's modified Eagle's medium (DMEM), penicillin-streptomycin, hygromycin-B, Zeocin, and Geneticin were purchased from Invitrogen (Carlsbad, CA). Fetal bovine serum (FBS) was purchased from Thermo Electron Corp. (Melbourne VIC, Australia). [^{3}H]NMS (82.0 Ci/mmol) and guanosine 5′-(γ-[^{35}S]thio)triphosphate ([^{35}S]GTPγS; 1250 Ci/mmol) were purchased from PerkinElmer Life and Analytical Sciences (Waltham, MA). McN-A-343 was purchased from Sigma/RBI (Natick, MA). C_7/3-phth was synthesized at the Institute of Drug Technology (Boronia, VIC, Australia), whereas AC-42 and 77-LH-28-1 were synthesized in-house at GlaxoSmithKline. Alcuronium chloride was a generous gift from F. Hoffmann-La Roche (Basel, Switzerland) and the SureFire cellular ERK1/2 assay kits were a generous gift from TGR BioSciences (Adelaide, Australia). AlphaScreen reagents were from PerkinElmer Life and Analytical Sciences. All other reagents were purchased from Sigma-Aldrich (St. Louis, MO) or BDH Merck (Victoria, Australia).

Receptor Mutagenesis. The coding sequence of the human M_2 mAChR, obtained from the UMR cDNA Resource Centre (http://www.cdna.org), was cloned into the gateway recombination entry vector, pENTR/D-TOPO, using the pENTR directional TOPO cloning kit (Invitrogen, Mt. Waverley, Australia) according to the manufacturer's instructions, after amplification of the gene using the following primers 5′-CACCATGAATAACTCAACAAACTCC-3′ (N-terminal forward primer with CACC sequence) and 5′-TTACCTTGTAGCGCCTATGTTC-3′ (C-terminal reverse primer). The native stop codon was subsequently mutated to Lys using the QuikChange Multi mutagenesis kit (Stratagene, La Jolla, CA), according to the manufacturer's instructions, before subcloning of the receptor into pEFS/FRT/V5-DEST gateway destination vector. Transfer of the M_2 mAChR from pENTR/D-TOPO into pEFS/FRT/V5-DEST was achieved using the LR Clonase enzyme mix kit (Invitrogen) and resulted in in-frame insertion of the V5 epitope tag at the C terminus of the receptor. This receptor sequence is referred to as "wild-type" throughout this study. Analysis of the properties of this clone after stable transfection in CHO cells revealed pharmacological properties equivalent to those of human M_2 mAChRs studied previously where the native stop codon was intact (Avlani et al., 2004). To study the influence of specific amino acids in receptor function, mutations were introduced into the wild-type receptor in pENTR/D-TOPO by site-directed mutagenesis using the QuikChange kit or QuikChange Multi kit (Y^{177}A + T^{423}A mutant). Mutant receptors were subsequently subcloned into the pEFS/FRT/V5-DEST vector as described above. Oligonucleotides for site-directed mutagenesis and DNA sequencing were purchased from GeneWorks (Hindmarsh, Australia). The primers used for the site-directed mutagenesis reactions are as follows: wild type (with V5 tag): 5′-CATAGGCGCTACAAGG***AAA***AAGGTGGGCGC-3′ (QuikChange Multi; single primer); ^{172}EDGE-^{175}-QNGQ: forward, 5′-GGGGTGAGAACTGTG***CAGAAT***GGG***CAG***TGCTACATTCAG-3′; reverse, 5′-CTGAATGTAGCA***CTG***CCC***ATTCTG***CACAGTTCTCACCCC-3′; Y^{177}A: 5′-GAGGATGGGGAGTGC***GCC***ATTCAGTTTTTTTCC-3′ (QuikChange Multi; single primer); T^{423}A: 5′-CCCAACACTGTGT***GGG***CAATTGGTTACTGGCTTTG-3′ (QuikChange Multi; single primer); ^{172}EDGE^{175}: QNGQ + Y^{177}A+-T^{423}A; forward, 5′-GGGGTGAGAACTGTG***CAGAAT***GGG***CAG***TGC***GCC***ATTCAG-3′; reverse, 5′-CTGAAT***GGC***GCA***CTG***CCC***ATTCTG***CACAGTTCTCACCCC-3′. Bold italic characters denote the nucleotides at which mutations were introduced. The integrity of all receptor clones was confirmed by cycle-sequencing with the ABI Prism BigDye Terminator v3.1 ready reaction cycle sequencing kit with reactions analyzed on an ABI Prism 373×I 96 capillary automated DNA sequencer (Australian Genome Research Facility, Parkville, Australia).

Transfections and Cell Culture. Wild-type and mutant receptors were isogenically integrated into CHO-FlpIn cells (Invitrogen) as follows: 75-cm^2 flasks with CHO FlpIn cells at 70 to 75% confluence were transfected in serum and antibiotic-free DMEM with 1 μg of pEFS/FRT/V5-DEST vector containing the wild-type or mutant M_2 mAChR gene and 9 μg of POG44 vector (containing Flp recombinase) using Lipofectamine (75 μl/75-cm^2 flask) according to the manufacturer's recommendations. Selection of cells expressing the receptors was achieved by treatment with 400 μg/ml hygromycin-B every 2 days until resistant floccules were obtained, before passaging a further five times. The cells were characterized for receptor expression by radioligand binding assay (see *Results*). Transfected and nontransfected CHO-FlpIn cells were grown and maintained in DMEM containing 20 mM HEPES, 10% fetal bovine serum, 50 U/ml penicillin-streptomycin, and 200 μg/ml Hygromycin-B (transfected CHO-FlpIn cells only) at 37°C in a humidified incubator containing 5% CO_2, 95% O_2.

[^{3}H]NMS Radioligand Binding Assay Membrane Preparation. When cells were approximately 90% confluent, they were harvested using trypsinization and centrifuged (300g, 3 min). The pellet was then resuspended in HEPES homogenization buffer (50 mM HEPES, 2.5 mM $MgCl_2$, and 2 mM EGTA), and the centrifugation procedure was repeated. The intact cell pellet was resuspended in HEPES homogenization buffer and homogenized using a homogenizer (Polytron; Kinematica, Littau-Lucerne, Switzerland) for two 10-s intervals at maximum setting, with 30-s cooling periods on ice between each burst. The homogenate was centrifuged (1000g, 10 min, 25°), the pellet was discarded, and the supernatant was recentrifuged (30,000g, 30 min, 4°C). The resulting pellet was resuspended in 5 ml of HEPES buffer (110 mM NaCl, 5.4 mM KCl, 1.8 mM $CaCl_2$, 10 mM $MgSO_4$, 25 mM glucose, 50 mM HEPES, and 58 mM sucrose, pH 7.4), and the protein content was determined using the method of Bradford (1976). The homogenate was then divided into 1-ml aliquots and stored frozen at −80°C until required for radioligand binding assays.

[^{35}S]GTPγS Assay Membrane Preparation. When cells were approximately 90% confluent, they were harvested using lifting buffer (10 mM HEPES, 0.9% NaCl, 0.2% EDTA, pH 7.4 at room temperature) and centrifuged (300*g*, 3 min). The pellet was then resuspended in buffer A (10 mM HEPES and 10 mM EDTA, pH 7.4, at 4°C) and homogenized as described above. The homogenate was centrifuged (5000*g*, 10 min, 4°C), the pellet was discarded, and the supernatant was recentrifuged (30,000*g*, 30 min, 4°C). The pellet was resuspended in buffer B (10 mM HEPES and 0.01 mM EDTA, pH 7.4 at 4°C) and centrifuged (30,000*g*, 30 min, 4°C). The resulting pellet was resuspended in 3 ml of buffer B, the protein content was determined, and aliquots were stored as described above

[^{3}H]NMS Inhibition or Potentiation Binding Assays. Membrane homogenates (25 μg) were incubated in a 1-ml total volume of Tris buffer (50 mM Tris Base, 3 mM $MgCl_2$, and 0.2 mM EGTA, pH 7.4) containing [^{3}H]NMS (0.5 nM) and a range of concentrations of gallamine, alcuronium, C_7/3-phth, acetylcholine, McN-A-343, AC-42, or 77-LH-28-1 at 37°C for 60 min (agonists) or 90 min (prototypical allosteric modulators), unless otherwise indicated under *Results*. Nonspecific binding was defined using 10 μM atropine. Incubation was terminated by rapid filtration through Whatman GF/B filters using a cell harvester (Brandel, Gaithersburg, MD). Filters were washed three times with 3-ml aliquots of ice-cold 0.9% NaCl buffer and dried before the addition of 4 ml of scintillation cocktail (Ultima Gold; PerkinElmer Life and Analytical Sciences). Vials were then left to stand until the filters became uniformly translucent before radioactivity was determined using scintillation counting.

[^{3}H]NMS Dissociation Kinetic Assay. CHO-FlpIn cell membranes (25 μg) were equilibrated with [^{3}H]NMS (0.5 nM) in a 1-ml total volume of Tris buffer (also containing 100 μM Gpp(NH)p for the McN-A-343 experiments) for 60 min at 37°C. Atropine (10 μM) alone or in the presence of test (allosteric) ligand was then added at various time points to prevent the reassociation of [^{3}H]NMS with the receptor. In subsequent experiments designed to investigate the effect of a range of modulator concentrations on [^{3}H]NMS dissociation rate, a "two-point kinetic" experimental paradigm was used, in which the effect of increasing concentrations of allosteric modulator on [^{3}H]NMS dissociation was determined at 0 and 6 min. This approach is valid to determine [^{3}H]NMS dissociation rate constants if the full time course of radioligand dissociation is monophasic in both the absence and the presence of modulator (Lazareno and Birdsall, 1995; Kostenis and Mohr, 1996); this was the case in our current study. The assays involved initial equilibration of CHO-FlpIn cell membranes (125 μg/ml) with [^{3}H]NMS (2.5 nM) in the presence or absence of atropine (100 μM) at 37°C for 1 h. For determination of radioligand dissociation at 6 min, equilibrated membrane/radioligand (100 μl) was added to Tris buffer containing atropine (100 μM) alone or in the presence of increasing concentrations of allosteric modulator to a 500 μl final volume. To determine radioligand binding at 0 min and nonspecific radioligand binding, 100 μl of membrane/radioligand equilibrated in the presence of absence of atropine was added to tubes alone. Termination of the reaction and determination of radioactivity were performed as described above.

[^{3}H]NMS Pseudo-Equilibrium Binding Assay. Two sets of tubes containing Tris buffer in the presence of McN-A-343 (0.3 nM–3 mM) or atropine (3 pM–10 μM), in the absence or presence of 100 μM Gpp(NH)p, were prepared to a 1-ml total volume. In each case, the first set of tubes was treated as per normal for standard radioligand binding assays; i.e., the reactants were added together and allowed to approach equilibrium. The second set of tubes was treated differently, whereby the orthosteric radioligand and receptor were pre-equilibrated at a high concentration, before dilution and exposure to allosteric ligand. In particular, to the first set of tubes, 10 μl of both [^{3}H]NMS (20 nM) and membrane (2500 μg/ml) were added separately (100-fold dilution). For the second set of tubes [^{3}H]NMS (20 nM) and membrane (2500 μg/ml), each representing 100× the desired final concentration, were first combined in a 1:1 ratio (thus reducing the concentration to 50× the desired final concentration), equilibrated for 30 mins at 37°, at which point 20 μl of the mixture was distributed to each tube, with the final result being a 50-fold dilution to the final desired concentration. Both sets of tubes were then incubated for 20 min at 37°C. Determination of nonspecific binding, termination of the reaction, and determination of radioactivity were performed as described above.

[^{3}H]GTPγS Binding Assay. Membrane homogenates (15 μg) were equilibrated in a 900-μl total volume of [^{35}S]GTPγS assay buffer (10 mM HEPES, 100 mM NaCl, and 10 mM $MgCl_2$, pH 7.4, at 30°C) containing 10 μM GDP and a range of concentrations of acetylcholine (0.3 nM–100 μM), pilocarpine (3 nM–300 μM), or McN-A-343 (3 nM–300 μM) at 30°C for 30 min. After this time, 100 μl of [^{35}S]GTPγS (100 pM) was added and incubation continued for another 30 min at 30°C. Termination of reaction and determination of radioactivity were performed as described above.

ERK1/2 Phosphorylation Assay. Cells were seeded into 96-well plates at a density of 50,000 cells/well. After 4 h, cells were washed twice with PBS and maintained in DMEM containing 20 mM HEPES and 50 U/ml penicillin-streptomycin for at least 4 h before assaying. Assays investigating the time course of action and concentration-response curves were generated by the addition of ligand for the indicated time periods (200-μl final volume) at 37°C. The time of stimulation for concentration-response curves represents the time of peak response as determined in time course assays. Agonist stimulation of cells (5 min unless otherwise specified) was terminated by the removal of media and the addition of 100 μl of SureFire lysis buffer to each well. The plate was then agitated for 1 to 2 min. A 4:1 (v/v) dilution of lysate/SureFire activation buffer was made in a total volume of 50 μl. A 1:100:120 (v/v/v) dilution of AlphaScreen beads/activated lysate mixture/*SureFire* reaction buffer in a 11-μl total volume was then transferred to a white opaque 384-well Proxiplate in diminished light. This plate was then incubated in the dark at 37°C for 1.5 h after which time the fluorescence signal was measured by a Fusion-α plate reader (PerkinElmer Life and Analytical Sciences), using standard AlphaScreen settings. All data were expressed as a percentage of the ERK1/2 phosphorylation mediated after a 6-min exposure to DMEM containing 3% FBS.

Data Analysis. Data sets of total and nonspecific binding obtained from each [^{3}H]NMS saturation binding assay were globally fitted to the following equation using Prism 4.03 (GraphPad Software, San Diego, CA).

$$Y = \frac{B_{\max} \times [\mathrm{A}]}{[\mathrm{A}] + K_{\mathrm{A}}} + NS \times [\mathrm{A}] \tag{1}$$

where Y represents radioligand binding, [A] denotes the concentration of radioligand, B_{max} denotes the maximal density of binding sites, K_A is the radioligand equilibrium dissociation constant, and NS is the fraction of nonspecific binding. The hyperbolic term in this equation was not used when fitting the nonspecific binding data, whereas the parameter NS was shared between both total and nonspecific binding data sets (Motulsky and Christopoulos, 2004).

Agonist inhibition binding data were empirically fitted to either a one-site (eq. 2) or two-site/state (eq. 3) inhibition mass action curve using Prism 4.03:

$$Y = Bottom + \frac{Top - Bottom}{1 + 10^{(X - \mathrm{LogIC}_{50})}} \tag{2}$$

where *Top* is the specific binding of the radioligand in the absence of any competing ligand, *Bottom* is the specific binding of the radioligand equal to nonspecific binding, IC_{50} is the concentration of competing ligand that produces radioligand binding halfway between the *Top* and *Bottom*, and X is the logarithm of the concentration of the competing ligand.

$$Y = Bottom + (Top - Bottom) \times \left(\frac{F_{\mathrm{H}}}{1 + 10^{X - \mathrm{LogIC}_{50_1}}} + \frac{1 - F_{\mathrm{H}}}{1 - 10^{X - \mathrm{LogIC}_{50_2}}}\right) \tag{3}$$

Y, Top, $Bottom$, and X are as above for eq. 2; F_H denotes the fraction of receptors inhibiting radioligand binding with a potency described by IC_{50_1}, whereas IC_{50_2} represents the inhibitory potency of the remaining fraction of receptors. In all instances, an extra-sum-of-squares (F test) was used to determine whether the data were better described by a one- versus a two-site model.

Dissociation kinetic data all followed a monoexponential decay and were thus fitted to the following equation using Prism 4.03:

$$B_t = B_0 \times e^{-k_{off} \times t} \quad (4)$$

where t denotes incubation time, B_t denotes specific radioligand binding at time t, B_0 denotes the specific radioligand binding at time at equilibrium (time = 0), and k_{off} represents the observed radioligand dissociation rate constant. For the two-point dissociation experiments, where the effects of a range of concentrations of allosteric modulators were investigated, individual k_{off} values determined in the presence of modulator were normalized to the control k_{off} value (absence of modulator) and then plotted as a function of modulator concentration. The EC_{50} value from the fit of a three-parameter logistic equation to these data represents the ratio K_B/α in the ATCM (Lazareno and Birdsall, 1995). In the case of the prototypical modulators gallamine, C_7/3-phth, and alcuronium, these two-point kinetic concentration response curves were globally (simultaneously) fitted with the corresponding pseudo-equilibrium binding curves (see below), with the parameters K_B and α shared between the data sets.

Pseudo-equilibrium binding data were analyzed by Prism 4.03 according to a kinetic ATCM (Lazareno and Birdsall, 1995; Avlani et al., 2004; Lanzafame et al., 2006). This model explicitly incorporates additional kinetic parameters, such as the dissociation rate constant of the radioligand in the absence and presence of allosteric modulator, and fits the binding as a function of incubation time.

$$B_t = B_{AB} \times [1 - e^{(-t \times k_{onobs})}] + B_{HI} \times e^{(-t \times k_{onobs})} \quad (5)$$

where

$$k_{onobs} = k_{offobx} \times \left(1 \times \frac{[A]}{K_{APP}}\right) \quad (6)$$

$$k_{offobs} = \frac{k_{off} + \dfrac{[B] \times k_{offB}}{(K_{B/\alpha})}}{1 + \dfrac{[B]}{(B_{AB/\alpha})}} \quad (7)$$

$$B_{AB} = \frac{[R]_t \times [A]/K_{APP}}{1 + [A]/K_{APP}} \quad (8)$$

$$B_{HI} + \frac{[R]_t \times [A] \times 50 \times 1/K_A}{1 + [A] \times 50 \times 1/K_A} \quad (9)$$

In these equations, B_t and t are as previously defined, [A] is the concentration of radioligand, k_{onobs} and k_{offobs} are the apparent radioligand association and dissociation rate constants in the presence of allosteric modulator, respectively, and k_{off} and k_{offB} denote the radioligand dissociation rate constants for the modulator-unoccupied and modulator-occupied receptor, respectively. t is the total concentration of receptors, B_{AB} denotes bound radioligand to both free and occupied receptor, and B_{HI} denotes the level of bound radioligand in the pre-equilibrated tubes. For tubes that are not pre-equilibrated, B_{HI} is equal to zero. K_{APP}, K_A, α, and [B] are as defined above. It is important to note that eqs. 5 to 9, based on the ATCM, assume that the measured effects of the allosteric ligand (i.e., modulation effects and any agonistic properties) arise via binding to a single (allosteric) site; if the ligand actually displays two different modes of binding (e.g., interacting with both the orthosteric and allosteric sites), then the ATCM will not yield correct estimates of the equilibrium binding properties of the modulator (May et al., 2007).

Agonist concentration-response curves were fitted to the following three-parameter-logistic equation using Prism 4.03.

$$Response = Bottom + \frac{(Top - Bottom)}{1 + 10^{(\mathrm{LogEC_{50}} - \mathrm{Log[A]})}} \quad (10)$$

where $Bottom$ and Top are the lower and upper plateaus, respectively, of the concentration-response curve, [A] is the molar concentration of agonist, and EC_{50} is the molar concentration of agonist required to generate a response halfway between the Top and $Bottom$.

For combination studies, the interaction between ACh and each of the partial allosteric agonists displayed high negative cooperativity (see *Results*) and therefore was indistinguishable from a competitive interaction. Consequently, ACh concentration response curves in the absence and presence of the partial agonists, McN-A-343, AC-42, and 77-LH-28-1, were adequately fitted to the following operational model for the competitive interaction between an orthosteric full agonist and orthosteric partial agonist, as derived previously by Leff et al. (1993).

$$E = \frac{E_m([A]K_B + \tau[B][EC_{50}])^n}{[EC_{50}]^n(K_B + [B])^n + ([A]K_B + \tau[B][EC_{50}])^n} \quad (11)$$

where E is the pharmacological effect, E_m is the maximal possible response, EC_{50} is the molar concentration of the orthosteric full agonist (A) required to achieve half-maximal response, n is the Hill slope of the orthosteric full agonist concentration-response curve, and K_B and τ represent the equilibrium dissociation constant and the operational index of efficacy of the partial agonist (B), respectively. This analysis assumes that 1) the values of E_m and n derived from the orthosteric full agonist concentration-response curve are approximate estimates of system maximal responsiveness and transducer function slope, respectively, and that 2) both agonists use the same transduction machinery and, as such, the Hill slope can be shared across the full and partial agonist concentration-response curves.

All affinity, potency, efficacy, and cooperativity parameters were estimated as logarithms (Christopoulos, 1998). In all instances, results are expressed as mean ± S.E.M. Statistical analyses were performed by a paired t test or by F test, as appropriate, using Prism 4.03, and statistical significance was taken as $p < 0.05$.

Results

Characterization of the Binding Properties of [^{3}H]NMS and Prototypical Allosteric Modulators at Wild-Type and Mutant M_2 mAChRs. Previous studies indicating a role for the M_2 mAChR residues ^{172}EDGE^{175}, Tyr^{177} and Thr^{423} in allosteric modulator binding generally used a substitution approach, whereby these amino acids in the M_2 mAChR (highest affinity for prototypical modulators) were swapped to corresponding amino acids in the M_5 mAChR (lowest affinity for prototypical modulators) to probe the determinants of modulator subtype-selectivity (see Introduction and references therein). In the current study, we created a different set of mutations in these regions. Specifically, we chose to investigate the impact of neutralizing the charge of the EDGE sequence while maintaining the side-chain structure [i.e., QNGQ ("M_2-EDGE" mutant), replacing Tyr^{177} and Thr^{423} with alanine ("M_2-YT" mutant) and a combination of the EDGE-QNGQ and Y^{177}A, T^{423}A mutations ("M_2-EDGE-YT" mutant)]. As expected, saturation binding assays using the orthosteric antagonist [^{3}H]NMS found no significant effects of any of the mutations on [^{3}H]NMS binding affinity relative to the wild-type ("M_2-WT") receptor (Table 1). Some variations were noted in the maximal density of binding sites (although all constructs were well expressed), but this was only statistically significant for the M_2-EDGE mutant (Table 1). In dissociation kinetic experiments, no significant differences were found for the dissociation rate of [^{3}H]NMS at any of the mutants relative to the wild type (0.29 ± 0.02 min^{-1}; n = 3). Thus, it can be concluded that the mutations did not significantly perturb the conformation of the orthosteric binding pocket or the access to or egress from that pocket by the radioligand.

In contrast, Fig. 2 illustrates the dramatic effects of the mutations on the ability of the prototypical modulators, alcuronium, gallamine, and C_7/3-phth to interact with [^{3}H]NMS in pseudo-equilibrium binding assays. Also shown are the effects of the modulators on [^{3}H]NMS dissociation

TABLE 1

Allosteric model binding parameters for the interaction between the orthosteric antagonist [^{3}H]NMS and each of three prototypical allosteric modulators at various M_2 mAChR mutants.

Values represent the mean ± S.E.M. from three to eight experiments performed in triplicate. pK_B is the negative logarithm of the equilibrium dissociation constant. B_{max} is the maximal density of binding sites. Log α is the logarithm of the cooperativity factor governing the allosteric interaction between the modulator and [^{3}H]NMS.

M_2 Receptor Construct	Orthosteric Ligand [^{3}H]NMS		Allosteric Modulator					
			Alcuronium		Gallamine		C_7/3-phth	
	pK_B	B_{max}	pK_B	Log α	pK_B	Log α	pK_B	Log α
		pmol/mg						
M_2-WT	9.20 ± 0.20	2.30 ± 0.30	5.96 ± 0.03	0.61 ± 0.03	5.95 ± 0.05	−1.55 ± 0.06	6.56 ± 0.03	−0.83 ± 0.03
M_2-EDGE	9.16 ± 0.36	1.00 ± 0.16*	5.56 ± 0.05*	0.64 ± 0.09	5.25 ± 0.05*	−1.26 ± 0.07	5.90 ± 0.04*	−0.63 ± 0.03*
M_2-YT	8.80 ± 0.12	2.93 ± 0.96	4.64 ± 0.07*	0.10 ± 0.02*	4.99 ± 0.06*	−1.54 ± 0.08	5.49 ± 0.04*	−0.97 ± 0.04
M_2-EDGE-YT	8.77 ± 0.28	3.15 ± 0.15	4.56 ± 0.05*	−0.18 ± 0.03*	4.43 ± 0.06*	−1.05 ± 0.07*	5.19 ± 0.04*	−0.84 ± 0.04

* Significantly different ($P < 0.05$) from the wild-type receptor as determined by one-way analysis of variance.

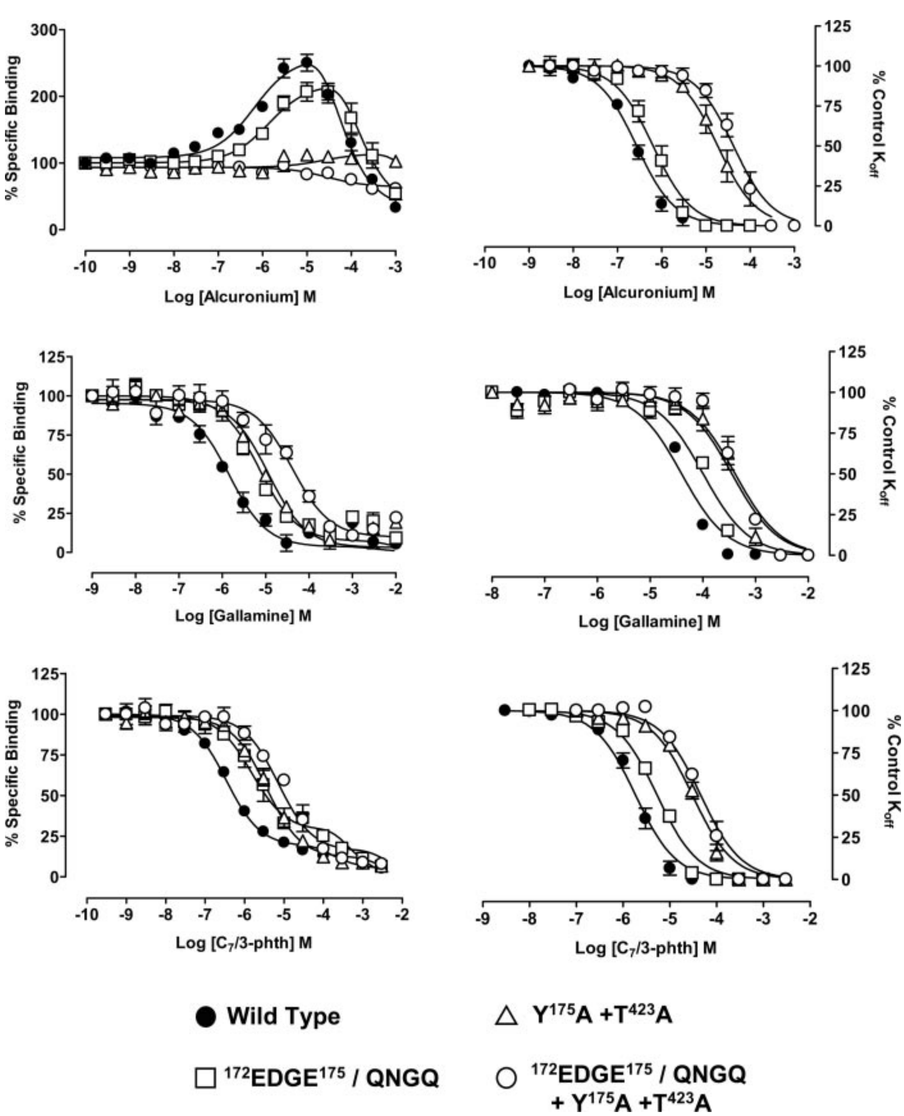

Fig. 2. Mutation of residues in the second extracellular loop/top of TM7 reduces the binding of prototypical M_2 mAChR allosteric modulators. The interaction between each prototypical modulator and the orthosteric ligand, [^{3}H]NMS (0.5 nM), was assessed at the M_2-WT and each of the indicated M_2 mAChR mutants using pseudo-equilibrium binding (left) or dissociation kinetic (right) assays at 37°C on membranes from CHO FlpIn cells. The curves superimposed on the data for each modulator represent the best global nonlinear regression curve fit of a kinetic ATCM to both the pseudo-equilibrium and dissociation kinetic experiments. Points represent the mean ± S.E.M. of three to eight experiments performed in triplicate.

kinetics. Global analysis of both groups of data to a kinetic ATCM yielded the parameters listed in Table 1. Removing the charge of the EDGE sequence while maintaining the essential side-chain structure significantly reduced the affinity of the allosteric enhancer alcuronium as well as that of the allosteric inhibitors gallamine and C_7/3-phth. The M_2-YT mutant had an even more profound inhibitory effect on modulator affinity. Not surprisingly, the combination of both sets of mutations had the strongest inhibitory effect on modulator affinity. In some instances, the cooperativity between each modulator and [^{3}H]NMS was also significantly changed (Table 1). The combined effect of reductions in modulator affinity and, in some cases, cooperativity, is manifested in the dissociation kinetic assays, where the potency of the compounds to allosterically retard [^{3}H]NMS dissociation is reduced between 10- and 150-fold (Fig. 2). Despite the reduced potency, however, all modulators were still able to completely prevent [^{3}H]NMS dissociation at high concentrations (Fig. 2).

Effects of Orthosteric and Allosteric Agonists on [^{3}H]NMS Inhibition Binding at the M_2-WT and M_2-EDGE-YT mAChRs. Given that the combined M_2-EDGE-YT mutation yielded the most profound reduction in the affinity of prototypical allosteric modulators, this receptor was chosen for comparison with the M_2-WT to investigate the effects on agonist binding. As shown in Fig. 3, the orthosteric agonist ACh, as well as McN-A-343, AC-42, and 77-LH-28-1, caused full inhibition of [^{3}H]NMS (0.5 nM) specific binding at both the M_2-WT and M_2-EDGE-YT mAChRs. These experiments were performed in the absence of any guanine nucleotides and, as such, it was expected that they could be influenced by the G protein-coupling status of the receptor. At both the M_2-WT and M_2-EDGE-YT, nonlinear regression of the ACh and McN-A-343 inhibition curves according to empirical binding models yielded Hill slopes that were significantly less than 1 and therefore preferentially fitted to an empirical two-site binding model (Table 2). Global nonlinear regression analysis of the ACh curves in conjunction with an extra-sum-of-squares test (F test) indicated that these curves were preferentially described by a single shared value for the fraction of receptors exhibiting high-affinity binding. At the M_2-EDGE+YT, ACh had a reduced apparent dissociation constant for the high-affinity, presumably G protein-coupled, form of the receptor; a similar trend was noted for the low-affinity binding site, but this was not statistically significant (Table 2). These results suggest that mutations

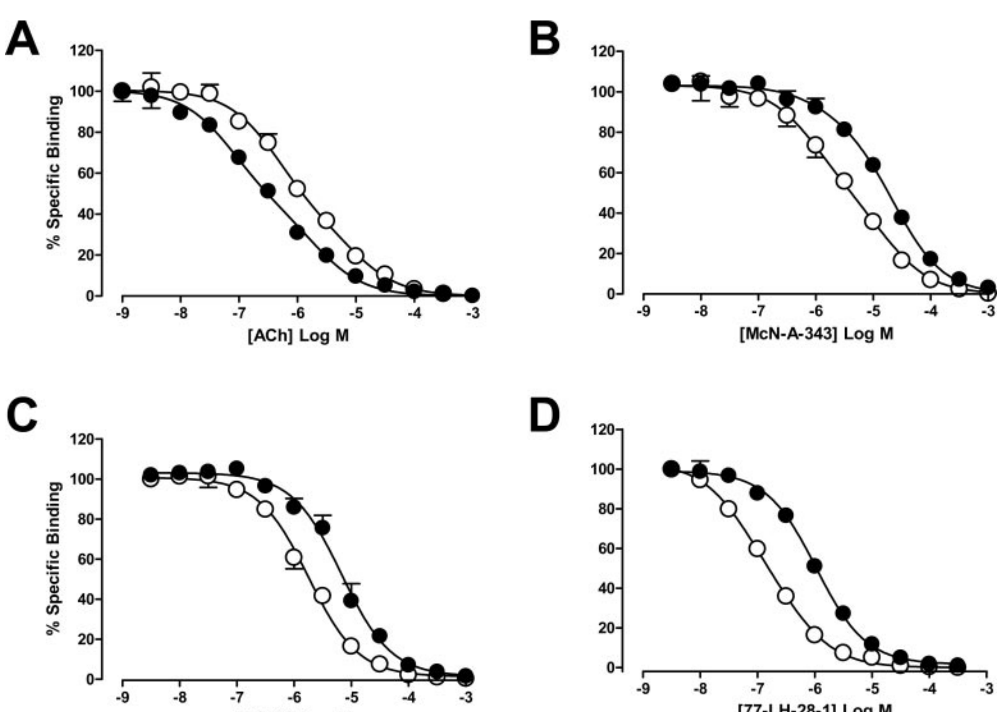

Fig. 3. Effects of the combined M_2-EDGE-YT mutations on the ability of mAChR agonists to inhibit the binding of [^{3}H]NMS. Inhibition of 0.5 nM [^{3}H]NMS binding at 37°C by ACh (A), McN-A-343 (B), AC-42 (C), or 77-LH-28-1 (D) at M_2-WT (●) and M_2-EDGE-YT (○) mAChRs in membranes from CHO FlpIn cells. The curves superimposed on the data points represent the best global fit of an empirical one- or two-site mass action binding model, as determined by an F test (see Table 2). In each case, data points represent the mean ± S.E.M. obtained from three experiments conducted in triplicate.

TABLE 2

Empirical inhibition binding parameters for ACh, McN-A-343, AC-42, and 77-LH-28-1 against [^{3}H]NMS at the M_2-WT and M_2-EDGE-YT mAChRs

Values represent the mean ± S.E.M. from three experiments performed in triplicate. $pK_{B(High)}$ and $pK_{B(Low)}$ are the negative logarithms of the apparent high- and low-affinity equilibrium dissociation constants, respectively, F_H is the fraction of the receptors exhibiting high-affinity binding, and n_H is the Hill slope.

	M_2-WT				M_2-EDGE-YT			
	$pK_{B(High)}$	$pK_{B(Low)}$	F_H	n_H	$pK_{B(High)}$	$pK_{B(Low)}$	F_H	n_H
ACh	7.08 ± 0.13	5.61 ± 0.17	0.59 ± 0.07	0.62 ± 0.06#	6.40 ± 0.12*	5.10 ± 0.16	0.59 ± 0.07	0.69 ± 0.08#
McN-A-343	6.14 ± 0.16	4.89 ± 0.08	0.15 ± 0.07	0.79 ± 0.07#	6.14 ± 0.16	4.89 ± 0. 08	0.51 ± 0.08*	0.67 ± 0.09#
AC-42		5.42 ± 0.06		0.98 ± 0.12		5.86 ± 0.05*		0.88 ± 0.08
77-LH-28-1		6.23 ± 0.03		0.91 ± 0.06	7.33 ± 0.11	5.73 ± 0.12	0.55 ± 0.06	0.82 ± 0.04#

Significantly different ($P < 0.05$) from 1.

* Significantly different ($P < 0.05$) from the corresponding control value within the same treatment group.

within the common allosteric site may actually have a small inhibitory effect on orthosteric agonist binding.

In contrast, global nonlinear regression analysis of the McN-A-343 binding curves in conjunction with an F test indicated that the data were best described by sharing both the high- and low-affinity dissociation constants of the two sites, but not the fraction of receptors exhibiting high affinity, which was found to be significantly *increased* at the M_2-EDGE+YT mAChR (Table 2). For AC-42, the inhibition of [^{3}H]NMS specific binding at both the wild-type and mutant receptor yielded Hill slopes that were not significantly different from 1, but the apparent equilibrium dissociation constant of AC-42 was modestly, but significantly ($p < 0.05$), increased at the M_2-EDGE+YT mAChR (Table 2). It is noteworthy that the inhibition of [^{3}H]NMS binding by 77-LH-28-1 preferentially fitted to a one-site model at the M_2-WT but a two-site binding model at the M_2-EDGE+YT mAChR (Table 2). Together, these results suggest that, in the absence of guanine nucleotides, the affinity of ACh seems to be slightly reduced, whereas McN-A-343, AC-42, and 77-LH-28-1 trend either toward an increased affinity or increased fraction of receptors exhibiting high affinity at the M_2-EDGE-YT mAChR.

Effects of McN-A-343, AC-42, and 77-LH-28-1 on [^{3}H]NMS Dissociation Kinetics at the M_2-WT and M_2-EDGE-YT mAChRs. To more directly probe the ability of McN-A-343, AC-42, and 77-LH-28-1 to allosterically modulate orthosteric ligand binding, the effect of these compounds on the rate of orthosteric radioligand dissociation was investigated. These experiments were all performed in the presence of 100 μM Gpp(NH)p to reduce receptor-G protein coupling and thus simplify the interpretation of the data. At the M_2-WT mAChR, the presence of McN-A-343 (300 μM; 0.17 $\pm$ 0.02 min^{-1}) and 77-LH-28-1 (100 μM; 0.15 $\pm$ 0.02 min^{-1}), but not AC-42 (100 μM; 0.22 $\pm$ 0.02 min^{-1}), significantly ($p <$ 0.05) retarded the dissociation rate of [^{3}H]NMS (Fig. 4A). These findings suggest that McN-A-343 and 77-LH-28-1 can bind simultaneously with [^{3}H]NMS to the M_2 mAChR to allosterically alter [^{3}H]NMS dissociation. At the M_2-EDGE-YT mAChR, 77-LH-28-1 (100 μM; 0.13 $\pm$ 0.06 min^{-1} versus 0.23 $\pm$ 0.02 min^{-1} for the wild-type) retained the ability to significantly retard [^{3}H]NMS dissociation; a trend was noted for McN-A-343 (0.17 $\pm$ 0.02 min^{-1}) as well, but this was not statistically significant at the concentration used (Fig. 4B). To more rigorously investigate the latter, the entire concentration-response relationship of McN-A-343 inhibition of [^{3}H]NMS dissociation kinetics was determined at both the wild-type and mutant mAChRs. At the M_2-WT, McN-A-343 caused virtually complete inhibition of [^{3}H]NMS dissociation (Fig. 4C) and the pEC$_{50}$ was determined as 3.23 $\pm$ 0.05 (n = 4). In contrast, at the M_2-EDGE-YT mAChR, McN-A-343 was unable to cause complete inhibition of [^{3}H]NMS dissociation kinetics and only had a small, albeit significant ($p < 0.05$), reduction in potency (pEC$_{50}$ = 2.98 $\pm$ 0.05; n = 4; Fig. 4C). This is in contrast to the effects on the prototypical modulators (Fig. 2), which were characterized by substantial reductions in allosteric potency but not maximal effect.

Quantification of the Allosteric Binding Properties of McN-A-343 at the M_2-WT and M_2-EDGE-YT mAChRs. The potency of McN-A-343 to retard the dissociation of [^{3}H]NMS in the kinetic assay reflects the combined effects of both modulator affinity (K_B) and cooperativity with the radioligand (α). To obtain individual estimates of the parameters, a different type of experiment is required. Because of the high negative cooperativity between [^{3}H]NMS and McN-A-343 (Fig. 3B), we exploited the ability of McN-A-343 to slow [^{3}H]NMS dissociation kinetics and to mediate a kinetic artifact in pseudo-equilibrium binding assays with reduced incubation times (20 min). These assays generate two curves, with the only variable between them being whether or not incubation was initiated by the addition of "free" (non pre-equilibrated) receptor or radioligand-bound (pre-equilibrated) receptor (see *Materials and Methods*). To ensure that orthosteric ligands do not mediate similar kinetic artifacts, these assays were initially performed using the classic orthosteric antagonist atropine. As shown in Fig. 5A for the M_2-WT mAChR, atropine yielded the expected behavior of a simple competitive orthosteric antagonist, causing complete inhibition of [^{3}H]NMS-specific binding irrespective of the order of ligand-receptor exposure. Nonlinear regression revealed that both curves preferentially fitted to a monophasic isotherm with a Hill slope not significantly different from

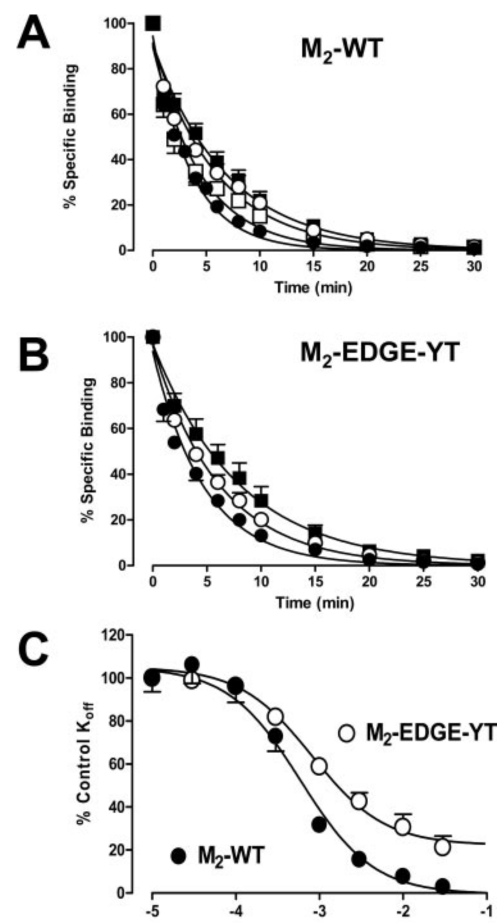

Fig. 4. Allosteric agonists can retard the dissociation rate of [^{3}H]NMS from the M_2 mAChR. [^{3}H]NMS dissociation determined in the absence (●) or presence of 300 μM McN-A-343 (○), 100 μM AC-42 (□), and 77-LH-28-1 (■) at 37°C to M_2-WT (●) (A) or M_2-EDGE-YT (○) (B) mAChRs in membranes from CHO FlpIn cells. C, full concentration-response relationship of the effect of McN-A-343 on the dissociation rate of [^{3}H]NMS at 37°C from the M_2-WT (●) and M_2-EDGE+YT (○) mAChRs. Data represent the mean $\pm$ S.E.M. obtained from three to five experiments conducted in duplicate.

one. When the Hill slope was constrained to one, the estimated pK_B values for atropine were 8.54 ± 0.03 and 8.47 ± 0.07 for non–pre-equilibrated and pre-equilibrated receptors, respectively (n = 3). In contrast, high concentrations of McN-A-343 [in the presence of 100 μM Gpp(NH)p], caused strikingly divergent effects on the approach of [^{3}H]NMS to equilibrium at both the M_2-WT (Fig. 5B) and the M_2-EDGE-YT (Fig. 5C) mAChRs, clearly indicating a stabilization of a ternary complex between receptor, radioligand, and high concentrations of McN-A-343 that leads to either an overestimation (pre-equilibration) or underestimation (no pre-equilibration) of the level of specific binding over the short assay time period relative to what would be obtained if the system were at equilibrium. A kinetic ATCM, which accounts for additional parameters such as the incubation time and the dissociation rates of [^{3}H]NMS from the modulator unoccupied and occupied receptor, was globally fitted to the curves to derive values of pK_B and Log α. Compared with the M_2 wild-type mAChR, the affinity of McN-A-343 for the M_2-EDGE-YT mAChR had significantly increased negative cooperativity (Log α of −1.40 ± 0.14 and −2.37 ± 0.05 for the M_2 WT and M_2-EDGE-YT mAChRs, respectively; n = 3) and a trend toward increased affinity (pK_B of 4.70 ± 0.17 and 5.10 ± 0.01 for the M_2-WT and M_2-EDGE-YT mAChRs, respectively; n = 3).

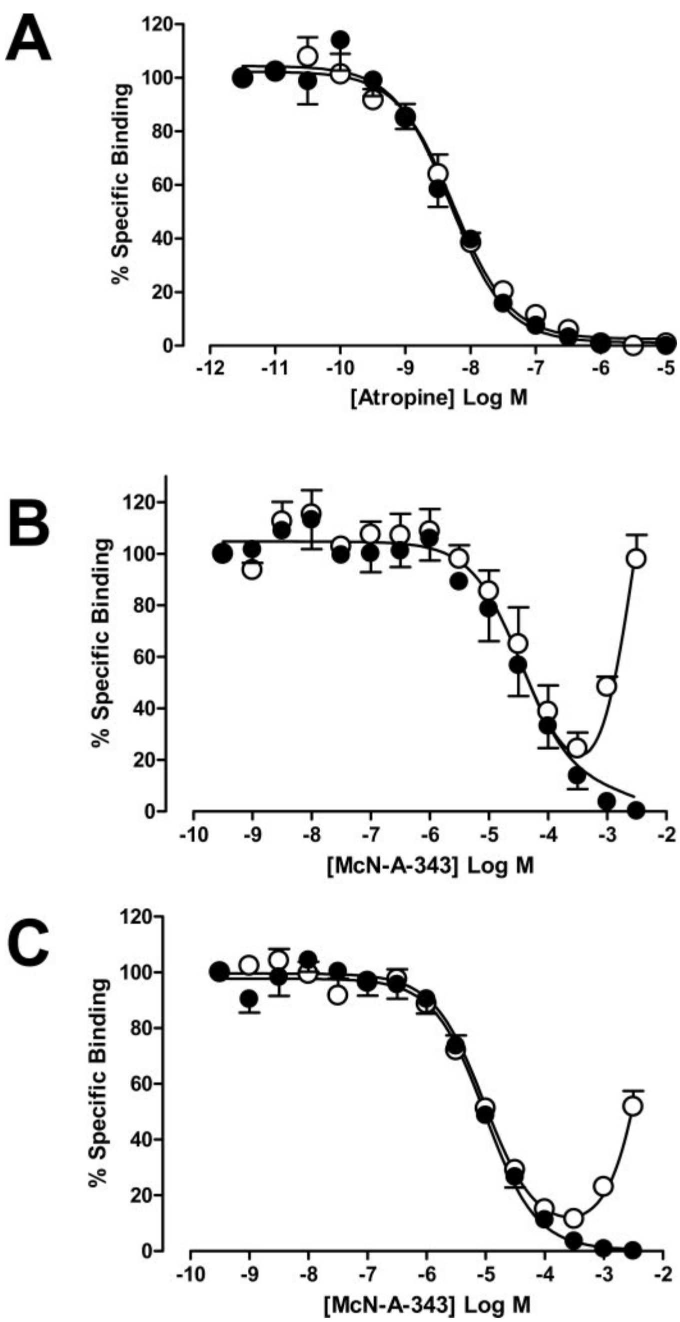

Fig. 5. McN-A-343 can cause kinetic binding artifacts on [^{3}H]NMS pseudo-equilibrium binding. M_2 mAChRs were either pre-equilibrated with [^{3}H]NMS before addition of unlabeled inhibitor (○) or exposed simultaneously to a high concentration of [^{3}H]NMS and inhibitor before dilution and incubation for an additional 20 min (●) at 37°C. Effects of atropine at M_2-WT mAChRs (A), McN-A-343 at M_2-WT mAChRs (B), and McN-A-343 at M_2-EDGE-YT MAChRs (C) in membranes from CHO FlpIn cells. Curves superimposed on the data represent the best global fit of a monophasic inhibition mass action curve (A) or a kinetic ATCM with the following parameter values: pK_A = 9.20; pK_B = 4.70 ± 0.17; Log α = −1.40 ± 0.14; k_{off} = 0.29 min^{-1}; k_{offB} = 0.002 min^{-1} (B); pK_A = 8.77; pK_B = 5.10 ± 0.01; Log α = −2.37 ± 0.05; k_{off} = 0.23 min^{-1}; k_{offB} = 0.04 min^{-1} (C). Values not associated with standard errors were determined in separate experiments and fixed as constants in the current analysis. In each case, data points represent the mean ± S.E.M. obtained from three experiments performed in triplicate.

Effects of Allosteric Site Mutations on Agonist Functional Properties. For initial functional experiments, the time course of ERK1/2 phosphorylation in response to orthosteric and allosteric agonists was determined in nontransfected, M_2-WT and M_2-EDGE-YT CHO-FlpIn cells. In addition to ACh, the partial agonist, pilocarpine, was included in these studies as a second well characterized orthosteric agonist. None of the ligands tested mediated a significant level of ERK1/2 phosphorylation in nontransfected CHO-FlpIn cells at any time points measured (data not shown). At both the M_2-WT and M_2-EDGE+YT mAChRs, ACh and pilocarpine mediated a robust stimulation, whereas AC-42 and 77-LH-28-1 mediated a very modest stimulation, of ERK1/2 phosphorylation (Fig. 6). Interestingly, the level of ERK1/2 phosphorylation mediated by McN-A-343 was markedly different at the M_2-WT and M_2-EDGE-YT mAChRs, with McN-A-343 causing only modest stimulation at M_2-WT mAChRs (Fig. 6A) but equivalent stimulation at the M_2-EDGE-YT mAChR to that obtained by ACh (Fig. 6B).

The time to the peak ERK1/2 phosphorylation was then chosen as the stimulation period for subsequent experiments aimed at characterizing orthosteric and allosteric concentration-response profiles at M_2-WT and M_2-EDGE-YT mAChRs. The orthosteric agonists, ACh and pilocarpine, mediated a robust stimulation of ERK1/2 phosphorylation at both M_2-WT and M_2-EDGE-YT mAChRs (Fig. 7A, 7B). Estimates of ACh potency and maximal response were not significantly different between the two receptors (Table 3). However, the maximal response elicited by pilocarpine was modestly but significantly ($p < 0.05$) increased at the M_2-EDGE-YT mAChR (Table 3); this likely reflects the slightly higher expression of the M_2-EDGE-YT mAChR compared with the M_2-WT receptor (Table 1). At the M_2-WT receptor, McN-A-343 and 77-LH-28-1 were weak partial agonists with respect to stimulation of ERK1/2 phosphorylation whereas AC-42 had minimal activity (Fig. 7A; Table 3). Interestingly, at the M_2-EDGE-YT mAChR, the efficacy of McN-A-343 was profoundly and significantly increased such that at this receptor it behaved as a full agonist (Fig. 7B; Table 3). Given the modest effect noted on pilocarpine maximal response, the

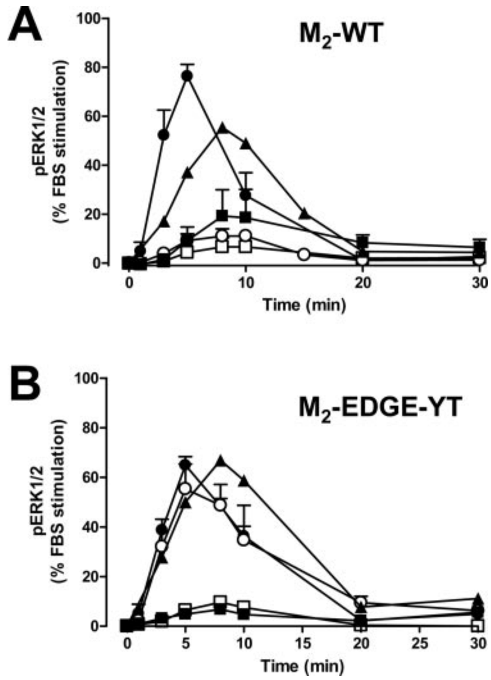

Fig. 6. Time course of M_2 mAChR-mediated ERK1/2 phosporylation. Effects of ACh (1 μM, ●), pilocarpine (100 μM, ▲), McN-A-343 (100 μM, ○), AC-42 (100 μM, □), and 77-LH-28-1 (100 μM, ■) on ERK1/2 phosphorylation at 37°C in CHO FlpIn cells stably expressing M_2-WT (A) or M_2-EDGE-YT mAChRs (B). Data points represent the mean ± S.E.M. obtained from three to six experiments conducted in duplicate, apart from pilocarpine, which is the mean from one experiment conducted in duplicate.

substantial increase in the efficacy of McN-A-343 is unlikely to simply reflect increased receptor expression. At the M_2-EDGE-YT mAChR, AC-42 maintained minimal activity whereas 77-LH-28-1 had a significantly increased potency (Fig. 7B; Table 3); because the latter compound remained a partial agonist, this increase in potency suggests an increase in affinity of 77-LH-28-1 at the mutant receptor. Thus, the functional results support the binding data in suggesting that mutations within the common allosteric site increase the affinity or efficacy of the allosteric agonists McN-A-343 and 77-LH-28-1.

To ensure that the functional effects of the receptor mutations were not influenced by any potential nonequilibrium artifacts associated with the ERK1/2 phosphorylation assay, a second assay measuring ligand mediated [^{35}S]GTPγS binding to activated G proteins was performed with the ligands pre-equilibrated before addition of the radiolabel. In this assay, ACh was a full agonist and pilocarpine a partial agonist at both the M_2-WT and M_2-EDGE+YT mAChRs (Fig. 7C, 7D). Similar to the ERK1/2 phosphorylation assays, McN-A-343 caused partial stimulation of [^{35}S]GTPγS binding at the M_2-WT mAChR but was practically indistinguish-

TABLE 3

Estimated potency (pEC_{50}) and maximal agonist effect (E_{max}) of mAChR agonists at mediating ERK1/2 phosphorylation

Values represent the mean ± S.E.M. obtained from 5 to 12 experiments performed in duplicate.

	M_2-WT	M_2-EDGE-YT	M_2-EDGE	M_2-YT
Acetylcholine				
pEC_{50}	7.52 ± 0.12	7.38 ± 0.12	7.64 ± 0.10	7.50 ± 0.09
E_{max}	90.8 ± 6.1	105.3 ± 4.3	77.1 ± 6.1	89.3 ± 5.6
Pilocarpine				
pEC_{50}	6.16 ± 0.24	5.66 ± 0.06	N.P.	N.P.
E_{max}	80.2 ± 5.6	108.3 ± 2.4*	N.P.	N.P.
McN-A-343				
pEC_{50}	5.35 ± 0.05	5.53 ± 0.12	5.10 ± 0.12	5.38 ± 0.11
E_{max}	18.0 ± 4.1	97.1 ± 4.3*	32.8 ± 8.1	68.0 ± 9.5*
AC-42				
pEC_{50}	N.D.	N.D.	N.D.	N.D.
E_{max}	N.D.	N.D.	N.D.	N.D.
77-LH-28-1				
pEC_{50}	5.87 ± 0.05	6.98 ± 0.15*	5.83 ± 0.53	6.78 ± 0.13*
E_{max}	16.8 ± 2.2	27.9 ± 4.7	13.43 ± 2.6	18.2 ± 3.0

N.D., value could not be accurately determined because of the very modest level of ERK1/2 phosphorylation; N.P., not performed

* Significantly different ($p < 0.05$) from the corresponding control value within the same treatment group.

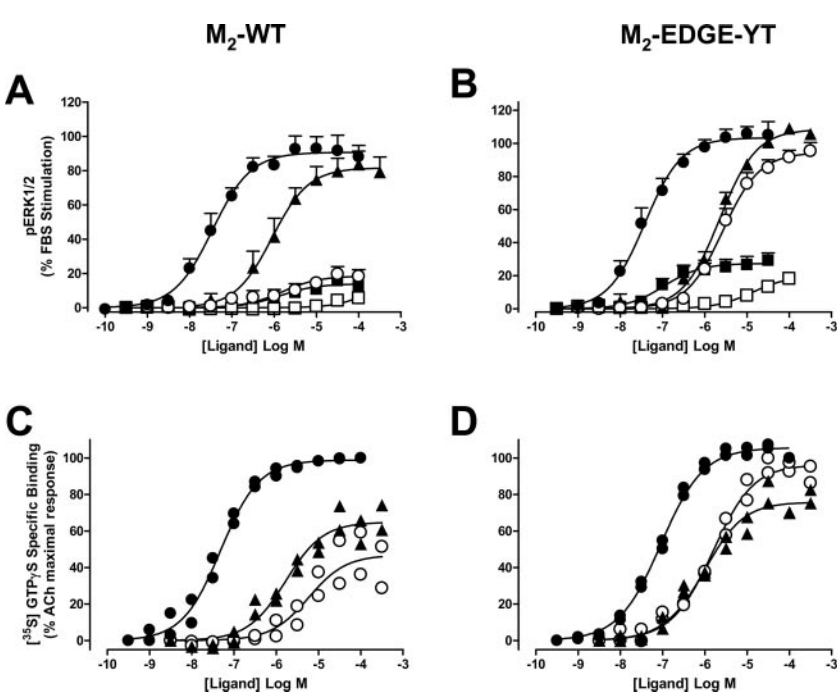

Fig. 7. Concordance between effects of M_2 mAChR mutation on allosteric agonism at two different signaling pathways. A and B, concentration-response curves to ACh (5-min stimulation, ●), pilocarpine (8-min stimulation, ▲), McN-A-343 (5-min stimulation, ○), AC-42 (8-min stimulation, □), and 77-LH-28-1 (8-min stimulation, ■) mediated ERK1/2 phosphorylation at 37°C in CHO FlpIn cells stably expressing the M_2-WT (A) or M_2-EDGE-YT (B) mAChRs. Data points represent the mean ± S.E.M. obtained from 6 to 12 experiments conducted in duplicate. C and D, concentration-response curves to ACh (●)-, pilocarpine (▲)-, and McN-A-343 (○)-mediated stimulation of [^{35}S]GTPγS binding to activated G proteins in FlpInCHO cell membranes stably expressing the M_2 wild-type (C) and M_2-EDGE+YT (D) mAChRs at 30°C. Data points represent individual means obtained from two experiments conducted in duplicate.

able from a full agonist at the M_2-EDGE-YT mAChR (Fig. 7C, 7D).

Finally, to determine which epitopes are primarily involved in mediating the effects of the combined M_2-EDGE-YT mutations, ERK1/2 phosphorylation assays were repeated using M_2-EDGE and M_2-YT mAChRs. At both receptors, ACh mediated a robust stimulation of ERK1/2 phosphorylation with no significant difference in potency or efficacy compared with the M_2-WT mAChR (Fig. 8 and Table 3). At the M_2-EDGE mAChR, the potency and efficacy of McN-A-343, AC-42 and 77-LH-28-1 were not significantly different from the M_2-WT mAChR (Fig. 8A and Table 3). However, the efficacy of McN-A-343 and the potency of 77-LH-28-1 were significantly increased at the M_2-YT mAChR, similar to the M_2-EDGE-YT mAChR (Fig. 8B and Table 3), suggesting that it is the two alanine substitutions that account for the majority of the effect. AC-42 had minimal activity at both the M_2-EDGE and M_2-YT mAChRs (Fig. 8).

Functional Interaction Studies between ACh and Allosteric Agonists at the M_2-WT and M_2-EDGE-YT mAChRs. In addition to gaining insight into the nature of the allosteric interaction, investigating the effect of allosteric modulators on orthosteric agonists can provide estimates of modulator affinity and, under appropriate conditions, cooperativity. McN-A-343, AC-42 and 77-LH-28-1 all mediated a parallel rightward shift in ACh mediated-ERK1/2 phosphorylation with no depression in the maximal response at either the M_2-WT (Fig. 9) or the M_2-EDGE-YT mAChR (Fig. 10; AC-42 and 77-LH-28-1 only); the interaction between McN-A-343 and ACh at the M_2-EDGE-YT mAChR was not investigated due to McN-A-343 acting as a full agonist at this receptor. Global fitting of the data sets to an operational model of competitive antagonism yielded Schild slopes that were not significantly different from 1 (Table 4), indicating that the interactions were characterized by very high negative cooperativity such that they were indistinguishable from a competitive (orthosteric) interaction. Therefore the data were re-fitted to the operational model with the Schild slope constrained to unity. The resulting pK_B estimates (Table 4) show that 77-LH-28-1 had a significantly increased affinity for the M_2-EDGE+YT mAChR, which agrees with the increased potency observed for 77-LH-28-1 in ERK1/2 phosphorylation concentration-response assays at the same mutant.

Discussion

We have found that the agonist McN-A-343 and the novel agonist 77-LH-28-1 have an allosteric mechanism of action at the human M_2 mAChR. A similar mechanism of action of AC-42 at the human M_2 mAChR could not be confirmed. Although we cannot yet conclude whether these agonists mediate all their effects via the allosteric site or whether they interact with both orthosteric and allosteric sites, the unique sensitivity of each of the compounds investigated to mutations within the common allosteric site on the M_2 mAChR strongly suggests that all these agonists have a different mode of binding compared with orthosteric ligands, such as ACh and pilocarpine, as well as prototypical mAChR modulators, such as gallamine, alcuronium, and C_7/3-phth. The enhanced activities of McN-A-343 and 77-LH-28-1 at mutant mAChRs that display reduced potencies for prototypical modulators was mediated mainly by the "common allosteric site" residues Tyr^{177} and Thr^{423} rather than ^{172}EDGE^{175}. To our knowledge, this is the first study investigating the effects of allosteric-site mutations on allosteric agonists of a family A GPCR.

Our finding that removal of the charge on ^{172}EDGE^{175} and substitution of Tyr^{177} and Thr^{423} with alanine led to a reduction in the potency of prototypical allosteric ligands (Fig. 2) is in agreement with previous studies (Leppik et al., 1994; Gnagey et al., 1999; Buller et al., 2002; Voigtländer et al., 2003; Huang et al., 2005) and confirms that these residues are vital to the binding of modulators structurally related to classic neuromuscular blockers and alkane-bis-onium compounds (Birdsall and Lazareno, 2005). In contrast, binding assays revealed no reduction in the potency of McN-A-343, AC-42, and 77-LH-28-1 to mediate complete inhibition of [^{3}H]NMS binding at both the M_2-WT and M_2-EDGE-YT mAChRs (Fig. 3). This finding suggested either that the agonists interacted competitively with [^{3}H]NMS, or that they interacted allosterically but with very high negative cooperativity. Previous studies of AC-42 and related compounds at M_1 mAChRs found similar evidence for high negative cooperativity with [^{3}H]NMS (Spalding et al., 2002, 2006; Langmead et al., 2006), as well as differential effects of orthosteric site mutations on these compounds compared with the orthosteric agonist carbachol (Spalding et al., 2002, 2006; Sur et al., 2003). In the current study, dissociation kinetic experiments provided conclusive evidence for an allosteric interaction at the human M_2 mAChR by McN-A-343 and 77-LH-28-1, but highlighted significant differences between the effects of allosteric-site mutations on allosteric agonist versus modulator binding. In particular, mutation of the key EDGE-YT residues in the common allosteric site caused approximately 10- to 150-fold reductions in the potency of prototypical modulators to retard [^{3}H]NMS dissociation (Fig. 3) but did not affect the ability of the modulators to completely retard radioligand dissociation. In contrast, the same mutations caused only a modest reduction in the potency of McN-

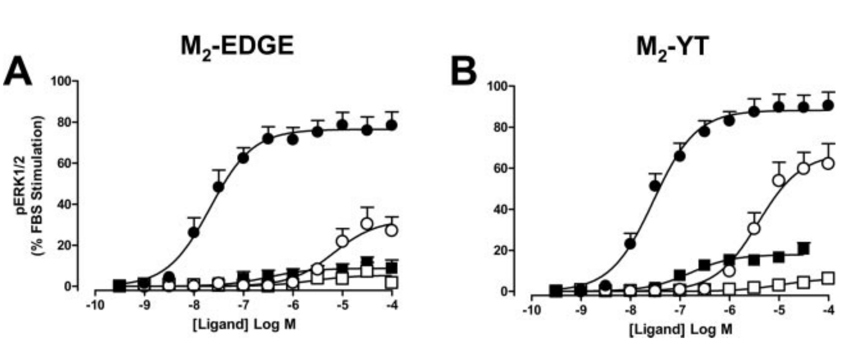

Fig. 8. Enhancement of the efficacy of McN-A-343 at mutant M_2 mAChRs is mediated mainly by the residues Tyr^{177} and Thr^{423}. Concentration-response curves to ERK1/2 phosphorylation mediated by ACh (5-min stimulation, ●), McN-A-343 (5-min stimulation, ○), AC-42 (8-min stimulation, □), and 77-LH-28-1 (8-min stimulation, ■) at 37°C in CHO FlpIn cells stably expressing the M_2-EDGE (A) or M_2-YT mAChRs (B). Data points represent the mean ± S.E.M. obtained from five to twelve experiments conducted in duplicate.

MOL PHARM

MOLECULAR PHARMACOLOGY

A-343 (approximately 1.8 fold), but led to a significant reduction in its maximal effect on radioligand dissociation rate (Fig. 4C).

In addition to the dissociation kinetic assays, our pseudo-equilibrium binding assays also provided evidence for an allosteric mode of interaction by McN-A-343, as well as yielding estimates of the affinity of McN-A-343 for the allosteric site and its cooperativity with [^{3}H]NMS. With the caveat that the pK_B and Log α values obtained from these assays are derived from a model that assumes McN-A-343 does not interact with the orthosteric site, the resulting estimates suggested that although there was no significant difference in the affinity of McN-A-343 for the mutant M_2 mAChR relative to the wild type, the modulator had significantly higher negative cooperativity with [^{3}H]NMS at the M_2-

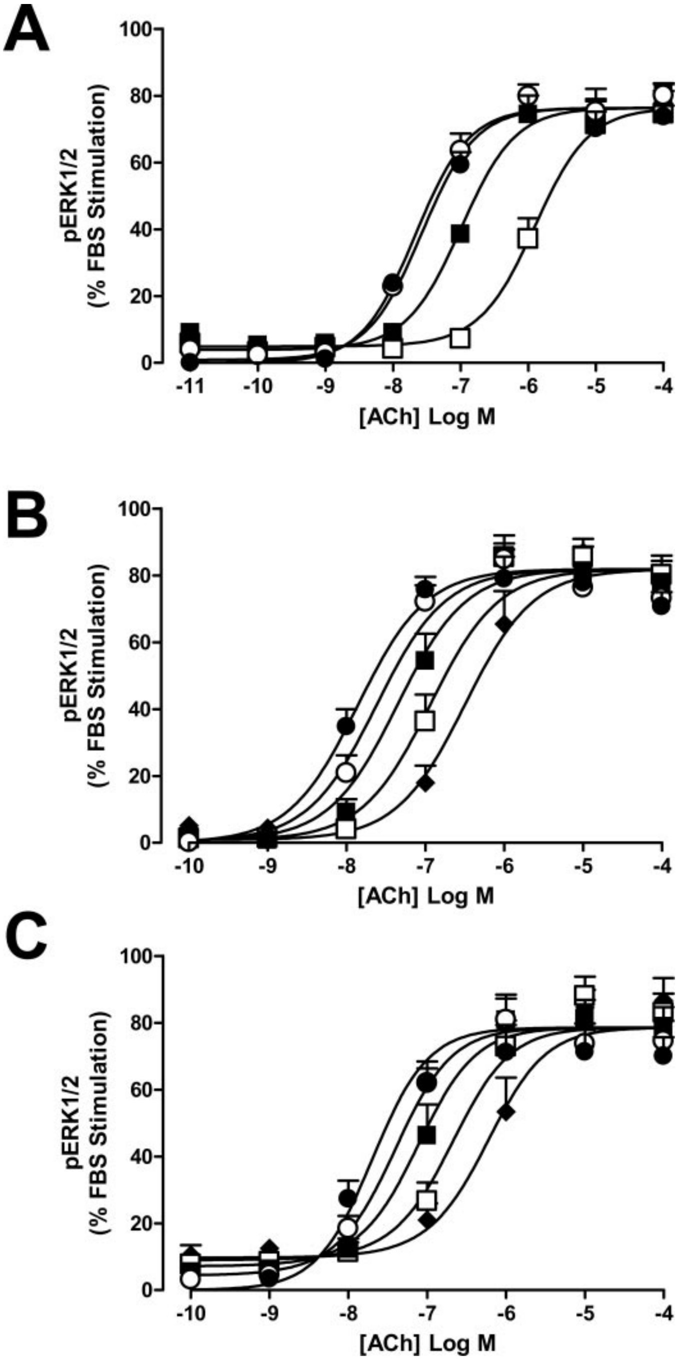

Fig. 9. Characterization of the interaction between ACh and allosteric agonists at M_2-WT mAChRs. ACh-mediated ERK1/2 phosphorylation in the absence (●) or presence of 10 μM (○), 100 μM (■), or 1 mM (□) McN-A-343 (A), 1 μM (○), 3 μM (■), 10 μM (□), or 30 μM (◆) AC-42 (B), or 77-LH-28-1 (C) at 37°C in CHO FlpIn cells stably expressing the M_2-WT mAChR. Curves superimposed on the data represent the best global fit of an operational model of competitive antagonism. Data points represent the mean ± S.E.M. obtained from five experiments conducted in duplicate.

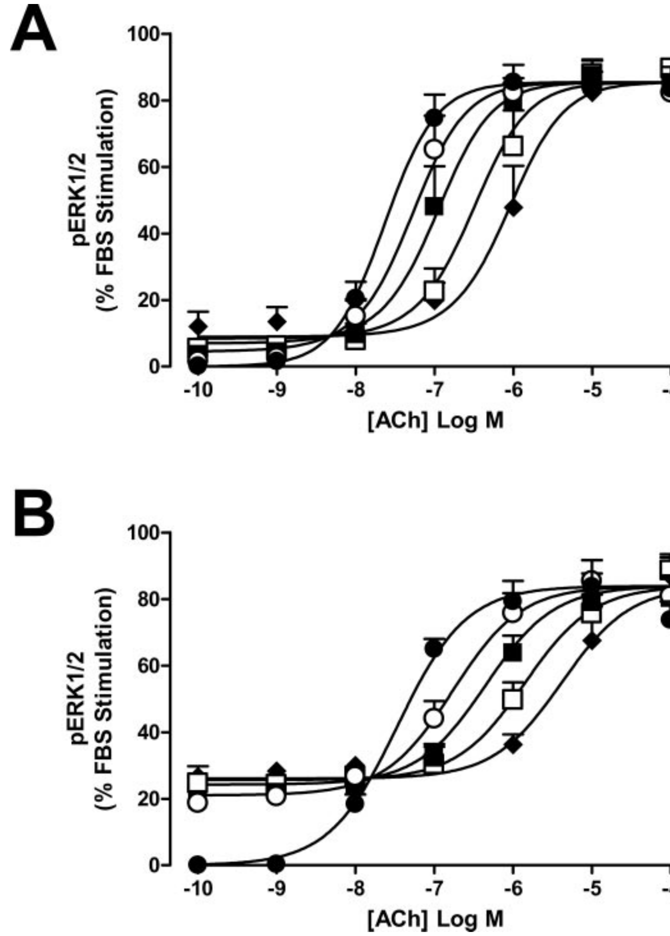

Fig. 10. Characterization of the interaction between ACh and allosteric agonists at M_2-EDGE-YT mAChRs. ACh-mediated ERK1/2 phosphorylation in the absence (●) or presence of 1 μM (○), 3 μM (■), 10 μM (□), or 30 μM (◆) AC-42 (A) or 77-LH-28-1 (B) at 37°C in CHO FlpIn cells stably expressing the M_2–EDGE-YT mAChR. Curves superimposed on the data represent the best global fit of an operational model of competitive antagonism. Data points represent the mean ± S.E.M. obtained from four experiments conducted in duplicate.

TABLE 4

Operational model pK_B and Schild slope estimates for McN-A-343, AC-42, and 77-LH-28-1 at the M_2-WT and M_2-EDGE-YT mAChRs from interaction studies with ACh in assays of ERK1/2 phosphorylation

Values represent the mean ± S.E.M. obtained from four to five experiments conducted in duplicate. pKB is the negative logarithm of the equilibrium dissociation constant, determined with the Schild slope constrained to equal 1

	M_2-WT		M_2-EDGE-YT	
	pK_B	Schild Slope	pK_B	Schild Slope
McN-A-343	4.69 ± 0.10	1.19 ± 0.12	N.P.	N.P.
AC-42	5.86 ± 0.11	0.92 ± 0.13	6.10 ± 0.13	1.15 ± 0.14
77-LH-28-1	5.95 ± 0.15	1.00 ± 0.16	6.44 ± 0.11*	0.97 ± 0.13

N.P., not performed.

* Significantly different ($P < 0.05$) from the corresponding control value at the same receptor.

EDGE-YT mAChR, consistent with a change in the mode of McN-A-343 binding. Taken together, the dissociation kinetic and pseudoequilibrium binding studies suggest that the ^{172}EDGE^{175}-QNGQ + Y^{177}A + T^{423}A mutations alter the binding of McN-A-343 and 77-LH-28-1 to the receptor in a manner that is different from classic (nonagonistic) modulators. It is likely that the allosteric agonists use different epitopes on the M_2 mAChR compared with the prototypical modulators, but it remains to be determined whether their binding site(s) overlap at all with the common allosteric site or whether the effects determined in the current study are mediated via indirect conformational changes transmitted between distinct allosteric sites.

Another interesting finding from the initial [^{3}H]NMS inhibition binding, assays conducted in the absence of Gpp(NH)p, was the effect of the combined allosteric-site mutation EDGE+YT on agonist affinity estimates. ACh, like many full agonists, displayed two apparent dissociation constants when competing with [^{3}H]NMS; the effect of the allosteric-site mutations was to reduce the potency of ACh somewhat, but McN-A-343, 77-LH-28-1, and AC-42 all trended toward either a higher affinity or an increase in the proportion of receptors demonstrating high-affinity binding. At the moment, it remains difficult to interpret the mechanistic basis of multiple agonist affinity states in competition binding studies, although in most instances it is assumed to reflect the G protein-coupling status to some extent (Christopoulos and El-Fakahany, 1999). If so, the findings from these types of binding assay indicated that mutation of the common allosteric site on the M_2 mAChR may actually increase the efficacy and/or potency of allosteric agonists, a hypothesis that could be directly tested in functional assays.

In experiments measuring M_2 mAChR-mediated ERK1/2 phosphorylation, both ACh and pilocarpine mediated a robust response, with potencies that were not significantly different between the M_2-WT and M_2-EDGE-YT receptors. Different results were obtained with McN-A-343, 77-LH-28-1, and AC-42, however, supporting the hypothesis that the binding mode of these agonists is unlikely to be the same as that of classic orthosteric ligands. The finding that McN-A-343, 77-LH-28-1, and AC-42 mediated minimal or no stimulation of ERK1/2 phosphorylation at the M_2-WT mAChR is consistent with the high functional selectivity of these compounds for the M_1 mAChR (Mitchelson, 1988; Spalding et al., 2002; C. J. Langmead, C. Bock-Zeigler, C. L. Branch, J. T. Brown, K. A. Buchanan, C. H. Davies, I. T. Forbes, V. A. H. Fry, J. J. Hagan, H. J. Herdon, et al., manuscript in preparation). At the M_2-EDGE-YT mAChR, the trend toward a modestly increased maximal response observed for pilocarpine, AC-42, and 77-LH-28-1 is likely to be a consequence of the slightly increased expression of the M_2-EDGE-YT mAChR (Table 1) as opposed to an enhanced intrinsic efficacy of each of the ligands. The most significant changes observed at the M_2-EDGE-YT mAChR were an increase of more than 5-fold in the maximal response (efficacy) of McN-A-343, such that at the mutant mAChR, it was a full agonist, and an increase of more than 10-fold in the potency of 77-LH-28-1; because the latter remained a partial agonist, the change in its potency must reflect a significant increase in its affinity for the M_2-EDGE-YT. These effects are qualitatively consistent with effects noted in the binding assays and are not assay-specific, because a similar profile was noted for McN-A-343 relative to ACh and pilocarpine in assays of [^{35}S]GTPγS binding to activated G proteins. Together, these results suggest that the conformation of the M_2-EDGE-YT mAChR, although having minimal effects on the function of orthosteric agonists, can have a profound effect on the efficacy (McN-A-343) or affinity (77-LH-28-1) of allosteric agonists. They also suggest that differences may exist between the binding/activation modes of McN-A-343 on the one hand and 77-LH-28-1 on the other. Experiments focusing on additional mutants, namely M_2-EDGE^{175}- versus M_2-YT, found that the latter alanine substitutions are likely to mediate the bulk of the observed effects on the allosteric agonists (Fig. 8).

Given that McN-A-343 and 77-LH-28-1 had an allosteric mechanism of action, it was also important to investigate the propensity for functional interaction between these compounds and the endogenous ligand ACh. In all instances, McN-A-343, 77-LH-28-1, and AC-42 displayed high negative cooperativity (α approaches 0 in the ATCM) with ACh at the M_2-WT and, as such, were fitted to a competitive (orthosteric) model describing the interaction of a partial agonist against a full agonist (Leff et al., 1993); this model is equivalent to the ATCM when $\alpha = 0$. As expected, the affinity of 77-LH-28-1 as an antagonist of ACh-mediated responses was significantly increased at the M_2-EDGE-YT mAChR. It is noteworthy that the affinity of AC-42 was only slightly increased, suggesting perhaps subtle differences in its binding mode relative to 77-LH-28-1. Unfortunately, the full agonism of McN-A-343 at the mutant receptor precluded the use of this agonist in similar interaction studies.

In conclusion, we have shown that McN-A-343 and 77-LH-28-1 exhibit both allosteric modulation and agonism at the human M_2 mAChR. In addition, we identified strikingly different effects that ^{172}EDGE^{175}-QNGQ, Y^{177}A, and T^{423}A allosteric-site mutations have on allosteric agonist compared with prototypical M_2 mAChR modulators, such as gallamine, alcuronium and C_7/3-phth. The growing list of allosteric modulators that possess intrinsic efficacy in their own right suggests that GPCRs may be activated from different regions within the receptor in addition to the orthosteric binding site. Given the potentially greater sequence diversity for receptor regions located outside the endogenous ligand-binding site, such allosteric agonists represent a new and exciting avenue for therapeutic intervention.

References

Avlani VA, May LT, Sexton PM, and Christopoulos A (2004) Application of a kinetic model to the apparently complex behaviors of negative and positive allosteric modulators of muscarinic acetylcholine receptors. *J Pharmacol Exp Ther* **308:**1062–1072.

Birdsall NJ and Lazareno S (2005) Allosterism at muscarinic receptors: ligands and mechanisms. *Mini-Rev Med Chem* **5:**523–543.

Birdsall NJM, Burgen ASV, Hulme EC, Stockton JM, and Zigmond MJ (1983) The effect of McN-A-343 on muscarinic receptors in the cerebral cortex and heart. *Br J Pharmacol* **78:**257–259.

Bradford MM (1976) A rapid and sensitive method for the quantitation of microgram quantities of protein utilizing the principle of protein-dye binding. *Anal Biochem* **72:**248–254.

Buller S, Zlotos DP, Mohr K, and Ellis J (2002) Allosteric site on muscarinic acetylcholine receptors: A single amino acid in transmembrane region 7 is critical to the subtype selectivities of caracurine V derivatives and alkane-bisammonium ligands. *Mol Pharmacol* **61:**160–168.

Christopoulos A (1998) Assessing the distribution of parameters in models of ligand-receptor interaction: to log or not to log. *Trends Pharmacol Sci* **19:**351–357.

Christopoulos A (2002) Allosteric binding sites on cell-surface receptors: novel targets for drug discovery. *Nat Rev Drug Discov* **1:**198–210.

Christopoulos A (2007) Muscarinic acetylcholine receptors in the central nervous system: Structure, function and pharmacology, in *Exploring The Vertebrate Central Cholinergic System* (Karczmar A ed) pp 163–208, Springer, New York.

Christopoulos A and El-Fakahany EE (1999) Qualitative and quantitative assessment of relative agonist efficacy. *Biochem Pharmacol* **58:**735–748.

Christopoulos A, Lanzafame A, and Mitchelson F (1998) Allosteric interactions at muscarinic cholinoceptors. *Clin Exp Pharmacol Physiol* **25:**185–194.
Eglen RM, Choppin A, and Watson N (2001) Therapeutic opportunities from muscarinic receptor research. *Trends Pharmacol Sci* **22:**409–414.
Ehlert FJ (1988) Estimation of the affinities of allosteric ligands using radioligand binding and pharmacological null methods. *Mol Pharmacol* **33:**187–194.
Ellis J, Huyler J, and Brann MR (1991) Allosteric regulation of cloned m1–m5 muscarinic receptor subtypes. *Biochem Pharmacol* **42:**1927–1932.
Felder CC, Bymaster FP, Ward J, and DeLapp N (2000) Therapeutic opportunities for muscarinic receptors in the central nervous system. *J Med Chem* **43:**4333–4353.
Gnagey AL, Seidenberg M, and Ellis J (1999) Site-directed mutagenesis reveals two epitopes involved in the subtype selectivity of the allosteric interactions of gallamine at muscarinic acetylcholine receptors. *Mol Pharmacol* **56:**1245–1253.
Huang XP, Prilla S, Mohr K, and Ellis J (2005) Critical amino acid residues of the common allosteric site on the M_2 muscarinic acetylcholine receptor: more similarities than differences between the structurally divergent agents gallamine and bis(ammonio)alkane-type hexamethylene-bis-[dimethyl-(3-phthalimidopropyl)ammonium]dibromide. *Mol Pharmacol* **68:**769–778.
Hulme EC, Birdsall NJM, and Buckley NJ (1990) Muscarinic receptor subtypes. *Annu Rev Pharmacol Toxicol* **30:**633–673.
Kostenis E and Mohr K (1996) Two-point kinetic experiments to quantify allosteric effects on radioligand dissociation. *Trends Pharmacol Sci* **17:**280–283.
Langmead CJ and Christopoulos A (2006) Allosteric agonists of 7TM receptors: expanding the pharmacological toolbox. *Trends Pharmacol Sci* **27:**475–481.
Langmead CJ, Fry VA, Forbes IT, Branch CL, Christopoulos A, Wood MD, and Herdon HJ (2006) Probing the molecular mechanism of interaction between 4-*n*-butyl-1-[4-(2-methylphenyl)-4-oxo-1-butyl]-piperidine (AC-42) and the muscarinic M_1 receptor: direct pharmacological evidence that AC-42 is an allosteric agonist. *Mol Pharmacol* **69:**236–246.
Lanzafame A, Christopoulos A, and Mitchelson F (1997) Three allosteric modulators act at a common site, distinct from that of competitive antagonists, at muscarinic acetylcholine M_2 receptors. *J Pharmacol Exp Ther* **282:**278–285.
Lanzafame AA, Sexton PM, and Christopoulos A (2006) Interaction studies of multiple binding sites on m4 muscarinic acetylcholine receptors. *Mol Pharmacol* **70:**736–746.
Lazareno S and Birdsall NJM (1995) Detection, quantitation, and verification of allosteric interactions of agents with labeled and unlabeled ligands at G protein-coupled receptors: interactions of strychnine and acetylcholine at muscarinic receptors. *Mol Pharmacol* **48:**362–378.
Lazareno S, Popham A, and Birdsall NJ (2000) Allosteric interactions of staurosporine and other indolocarbazoles with *N*-[methyl-^{3}H]scopolamine and acetylcholine at muscarinic receptor subtypes: identification of a second allosteric site. *Mol Pharmacol* **58:**194–207.
Leff P, Dougall IG, and Harper D (1993) Estimation of partial agonist affinity by interaction with a full agonist: a direct operational model-fitting approach. *Br J Pharmacol* **110:**239–244.
Leppik RA, Miller RC, Eck M, and Paquet JL (1994) Role of acidic amino acids in the allosteric modulation by gallamine of antagonist binding at the m2 muscarinic acetylcholine receptor. *Mol Pharmacol* **45:**983–990.
Matsui H, Lazareno S, and Birdsall NJ (1995) Probing of the location of the allosteric site on m1 muscarinic receptors by site-directed mutagenesis. *Mol Pharmacol* **47:**88–98.
May LT, Leach K, Sexton PM, and Christopoulos A (2007) Allosteric modulation of G protein-coupled receptors. *Annu Rev Pharmacol Toxicol* **47:**1–51.
Mitchelson F (1988) Muscarinic receptor differentiation. *Pharmacol Ther* **37:**357–423.
Motulsky HJ and Christopoulos A (2004) *Fitting Models to Biological Data Using Linear and Nonlinear Regression. a Practical Guide to Curve Fitting.* Oxford University Press, New York.
Prilla S, Schrobang J, Ellis J, Holtje HD, and Mohr K (2006) Allosteric interactions with muscarinic acetylcholine receptors: Complex role of the conserved tryptophan $M_2{}^{422}$Trp in a critical cluster of amino acids for baseline affinity, subtype selectivity, and cooperativity. *Mol Pharmacol* **70:**181–193.
Spalding TA, Ma JN, Ott TR, Friberg M, Bajpai A, Bradley SR, Davis RE, Brann MR, and Burstein ES (2006) Structural requirements of transmembrane domain 3 for activation by the M_1 muscarinic receptor agonists AC-42, AC-260584, clozapine, and *N*-desmethylclozapine: evidence for three distinct modes of receptor activation. *Mol Pharmacol* **70:**1974–1983.
Spalding TA, Trotter C, Skjaerbaek N, Messier TL, Currier EA, Burstein ES, Li D, Hacksell U, and Brann MR (2002) Discovery of an ectopic activation site on the M_1 muscarinic receptor. *Mol Pharmacol* **61:**1297–1302.
Sur C, Mallorga PJ, Wittmann M, Jacobson MA, Pascarella D, Williams JB, Brandish PE, Pettibone DJ, Scolnick EM, and Conn PJ (2003) *N*-desmethylclozapine, an allosteric agonist at muscarinic 1 receptor, potentiates *N*-methyl-D-aspartate receptor activity. *Proc Natl Acad Sci U S A* **100:**13674–13679.
Voigtländer U, Johren K, Mohr M, Raasch A, Trankle C, Buller S, Ellis J, Holtje HD, and Mohr K (2003) Allosteric site on muscarinic acetylcholine receptors: identification of two amino acids in the muscarinic M_2 receptor that account entirely for the M2/M5 subtype selectivities of some structurally diverse allosteric ligands in *N*-methylscopolamine-occupied receptors. *Mol Pharmacol* **64:**21–31.
Waelbroeck M (1994) Identification of drugs competing with d-tubocurarine for an allosteric site on cardiac muscarinic receptors. *Mol Pharmacol* **46:**685–692.
Zahn K, Eckstein N, Trankle C, Sadee W, and Mohr K (2002) Allosteric modulation of muscarinic receptor signaling: alcuronium- induced conversion of pilocarpine from an agonist into an antagonist. *J Pharmacol Exp Ther* **301:**720–728.

Address correspondence to: Prof Arthur Christopoulos, Drug Discovery Biology Laboratory, Department of Pharmacology, Monash University, Clayton, Victoria 3800, Australia. E-mail: arthur.christopoulos@med.monash.edu.au